Dynamical Breakup of the Fermi Surface in a Doped Mott Insulator

M. Civelli,[1] M. Capone,[2,3] S. S. Kancharla,[4] O. Parcollet,[5] and G. Kotliar[1]

[1]*Physics Department and Center for Materials Theory, Rutgers University, Piscataway New Jersey USA*
[2]*INFM-SMC and Istituto dei Sistemi Complessi CNR, Via dei Taurini 19, I-00185, Rome, Italy*
[3]*Physics Department, University of Rome "La Sapienza," Piazzale Aldo Moro 5, I-00185, Rome, Italy*
[4]*Departement de physique and Regroupement quebecois sur les materiaux de pointe, Université de Sherbrooke, Sherbrooke, Quebec, Canada J1K 2R1*
[5]*Service de Physique Theorique, CEA Saclay, 91191, Gif-Sur Yvette, France*

(Received 26 November 2004; revised manuscript received 12 May 2005; published 2 September 2005)

The evolution from an anomalous metallic phase to a Mott insulator within the two-dimensional Hubbard model is investigated by means of the cellular dynamical mean-field theory. We show that approaching the density-driven Mott metal-insulator transition the Fermi surface is strongly renormalized and the quasiparticle description breaks down in a very anisotropic fashion. Regions where the quasiparticles are strongly scattered (hot spots) and regions where the scattering rate is relatively weak (cold spot) form irrespective of whether the parent insulator has antiferromagnetic long-range order, while their location is not universal and is determined by the interplay of the renormalization of the scattering rate and the Fermi surface shape.

DOI: 10.1103/PhysRevLett.95.106402 PACS numbers: 71.10.Fd, 71.27.+a, 74.20.Mn, 79.60.−i

The discovery of high-temperature superconductivity has led to a revival of interest in the Mott transition (MT) problem [1]. The goal is to understand the evolution of the electronic structure of a strongly correlated electron system as a function of a control parameter, such as doping in a Mott insulator (MI). This problem has been addressed using a large number of numerical and analytical techniques, but a coherent picture of this phenomenon in two dimensions is still lacking.

In this Letter we study the two-dimensional Hubbard model on the square lattice:

$$H = -\sum_{i,j,\sigma} t_{ij}(c^{\dagger}_{i\sigma}c_{j\sigma} + \text{H.c.}) + U\sum_{i} n_{i\uparrow}n_{i\downarrow} - \mu\sum_{i} n_{i},$$

where $c_{i\sigma}$ ($c^{\dagger}_{i\sigma}$) are destruction (creation) operators for electrons of spin σ, $n_{i\sigma} = c^{\dagger}_{i\sigma}c_{i\sigma}$ is the number operator, U is the on-site repulsion, and μ is the chemical potential determining the electron density $n = (1/N)\Sigma_{i,\sigma}\langle n_{i\sigma}\rangle$ (N is the number of sites). The hopping amplitude t_{ij} is limited to nearest neighbors t and to next-nearest neighbors t'. We consider the strongly correlated regime taking $U = 16t$. Our study is confined to the hole-doped system ($n < 1$) at different levels of frustration controlled by the ratio t'/t. This is equivalent to the electron-doped system ($n > 1$) upon a particle-hole transformation that reverses the sign of t'. In particular, we take small values of $t'/t = \pm 0.3$ suitable to describe the cuprates and a large value $t'/t = 0.9$, chosen in order to completely frustrate the antiferromagnetism (AFM) [see the right panel of Fig. 1 displaying the staggered magnetization $m = (1/N) \times \Sigma_i(-1)^i(n_{i\uparrow} - n_{i\downarrow})$ at half-filling as a function of t'/t].

We investigate the MT in the normal state using a recently developed extension of dynamical mean-field theory (DMFT) [2], the cellular dynamical mean-field theory (CDMFT) [3]. CDMFT reduces a quantum lattice problem to a quantum impurity model consisting of a cluster of sites, in our case a 2×2 plaquette (see Fig. 1), embedded in an effective medium described by a self-consistently determined Weiss function. In this work we consider a metallic phase that does not break any symmetry and follow its evolution as a function of doping. The method, however, can describe various broken symmetries, such as AFM or d-wave superconductivity. Other extensions of single-site DMFT have been proposed and applied to both the normal and the broken-symmetry phases [4].

In this work, we gain new insights in the approach of the MT through the introduction of two technical advances: (i) the use of CDMFT, which provides a natural real-space description of the physics and allows for the introduction of k-dependent properties that extend the investigation of previous single-site DMFT studies [5], (ii) the solution of the impurity model by means of exact diagonalization (ED), following the single-site DMFT method of Ref. [6]. The advantage of ED is the access to zero temperature and real frequency information, as well as the ability to treat the large-U regime, which is hardly accessible by the quantum Monte Carlo (QMC) method. CDMFT on a plaquette describes the evolution of the electronic structure of the model in terms of just a few (three is the present case)

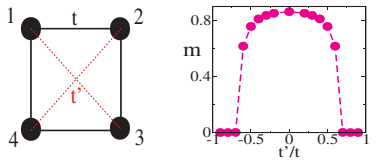

FIG. 1 (color online). Left side: the CDMFT plaquette. Right side: staggered magnetization as a function of the next-nearest hopping t' at half-filling. The parameter t' controls the magnetic frustration in the system.

functions of frequency, which have a simple physical interpretation as parametrizing the lattice self-energy, and which show a systematic evolution towards the MI (see Fig. 2 and discussion below). It can be thought of as a dynamical generalization of the early slave-boson mean-field theory [7], which is able to treat both the coherent and the incoherent excitations (quasiparticle peak and Hubbard bands) on the same footing.

In order to perform an ED solution, the quantum impurity model is truncated to a finite number (in this case 8) bath level, whose energies and hybridizations are self-consistently determined through a minimization procedure. To implement the self-consistency condition, we introduce Matsubara frequencies and hence an effective inverse temperature β, which we set to $\beta = 128$ in units of the half bandwidth $4t$. At low β and relatively small U our results are qualitatively similar to those obtained solving the impurity by QMC. Details on the implementation of ED within CDMFT and a benchmark against the exact solution of the Hubbard model in one dimension were presented in [8]. ED method's main limitations are the small number of sites in the bath and the effective temperature, which induce a limited energy resolution [8,9]. The small size of the cluster induces a finite k resolution: for the 2×2 plaquette with the square symmetry we have only two independent directions in k space (along the diagonal and along the lattice axis).

Our main results can be summarized as follows: (i) The Fermi surface (FS) shape is strongly renormalized by the interactions. For t'/t negative (reminiscent of hole-doped cuprates), approaching half-filling the absolute value of the renormalized t'/t increases, thereby enhancing the holelike curvature of the FS. On the other hand, for t'/t positive (reminiscent of the electron-doped cuprates), the effective t'/t becomes small close to the MI, and the system is driven toward a nested FS. (ii) The approach to the MI is characterized by the appearance of regions with very different electronic lifetimes. The interplay of this phenomenon of

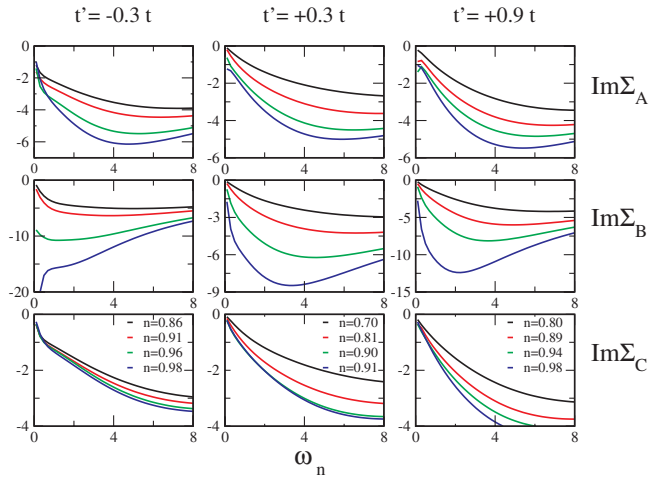

FIG. 2 (color online). Imaginary part of the eigenvalues of the cluster self-energies for $t'/t = \pm 0.3, +0.9$.

momentum-space differentiation and the renormalization of the FS determines the location of *hot or cold regions* that are observed in angle-resolved photoemission spectroscopy (ARPES) spectra [10] and in previous theoretical results [11,12]. (iii) The proximity of the MT is the fundamental ingredient that gives rise to momentum-space differentiation, rather than the proximity to a state with long-range AFM correlations. Indeed, t' as large as at $t' = 0.9t$, where AFM is destroyed already at half-filling, exhibits a momentum-space differentiation. The large t' results are similar to those for $t' = 0.3t$ at the k resolution used in this Letter.

Using the square symmetry, the CDMFT results for the plaquette are succinctly expressed in terms of three self-energies Σ_{11}, Σ_{12}, Σ_{13}, or alternatively in terms of the eigenvalues of the cluster self-energy matrix Σ_{ij}, which can be thought of as the lattice self-energies in specific points of the momentum space, namely $\Sigma_A = \Sigma_{11} - \Sigma_{13}$ in $(0, \pi)$ and $(\pi, 0)$, $\Sigma_{B[C]} = \Sigma_{11} - [+]2\Sigma_{12} + \Sigma_{13}$ in (π, π) $[(0, 0)]$. CDMFT causality requires that the imaginary part of all the self-energy eigenvalues is negative. We extract the momentum-space dependence of the electronic structure from the calculated cluster quantities using [11]

$$\Sigma_{\text{latt}}(k, \omega) = \Sigma_A S_A(k) + \Sigma_B S_B(k) + \Sigma_C S_C(k), \quad (1)$$

where the functions $S_A(k) = (1 - \cos k_x \cos k_y)/2$ and $S_{B[C]}(k) = (1 - [+]\cos k_x - [+]\cos k_y + \cos k_x \cos k_y)/4$ are positive. Other methods of periodization [13,14] do not change qualitatively the conclusions of this Letter.

As shown in Fig. 2, Σ_A, Σ_B, and Σ_C exhibit a clear systematic behavior as the MT is approached (we plot only the imaginary part, which we discuss in the following, but a similar behavior is followed by the real part). At large doping, only Σ_{11} is appreciably different from zero, while $\Sigma_{12}, \Sigma_{13} \simeq 0$. The lattice self-energy $\Sigma_{\text{latt}}(k, \omega)$ from Eq. (1) is therefore k-independent and single-site DMFT results are recovered. However, the cluster self-energies increase sizably at low doping, making Σ_{latt} strongly k dependent. The zero frequency limit of the real part of $\Sigma(k, \omega)$ determines the shape of the interacting FS, which we define as $t_{\text{eff}}(k) = \mu$, where $t_{\text{eff}}(k) \equiv t(k) - \text{Re}\Sigma_{\text{latt}}(k, \omega = 0^+)$, $t(k)$ being the Fourier transform of the hopping t_{ij} and the $\omega = 0^+$ limit is extrapolated from the lowest Matsubara frequency.

The renormalization of the FS becomes appreciable close to the MT. The self-energy itself depends weakly on the sign of t', and, in particular, it has the same sign for both positive and negative t'. However, given its large magnitude, when combined with t' of different signs, it produces interacting FS's of very different shapes in the electron-doped and hole-doped cases (dashed lines in Fig. 3). This can be understood in terms of the renormalized low energy hopping coefficients $t_{\text{eff}} = t - \text{Re}\Sigma_{12}(\omega = 0^+)/2$ and $t'_{\text{eff}} = t' - \text{Re}\Sigma_{13}(\omega = 0^+)/4$ presented in Fig. 4. Regardless of the value of t'/t, correlations act to *increase* the value of t_{eff}. This physical effect, predicted by earlier

slave-boson studies [7], reduces the mass divergence characteristic of single-site DMFT where the effective mass scales inversely proportionally to the quasiparticle residue. The renormalization of t' depends instead on the sign of t'/t. This is an effect that is not present in slave-boson theories [7]. For $t' = -0.3t$, $|t'_{\mathrm{eff}}|$ increases in such a way that the ratio $(t'_{\mathrm{eff}}/t_{\mathrm{eff}})/(t'/t)$ weakly increases approaching the MI, thereby enhancing the holelike curvature of the FS. On the other hand, t'_{eff} decreases for $t' = +0.3t$, giving rise to an almost nested FS as half-filling is approached. This is also clearly seen in Fig. 3, where the FS is shown on top of the spectral function (see below). In the hole-doped case we observe also a horizontal flattening of the FS close to $(0, \pi)$ or $(\pi, 0)$ approaching the MT. The shape of the FS is similar to that observed in ARPES [15], and thereby interpreted as resulting from a doping independent nesting vector.

Previous studies [5] based on a local approximation including spin fluctuations revealed that the approach to the MT is accompanied by a reduction of the coherence temperature (above which we have an incoherent metal with large $\mathrm{Im}\,\Sigma$) and the generation of incoherent states when $\mu_{\mathrm{eff}} = \mu - \mathrm{Re}\Sigma(\omega = 0)$ is out of the bare band of the original model. These properties appear in our study *but only in parts of the Brillouin zone,* because of the phenomenon of momentum-space differentiation: quasiparticles disappear in some regions of momentum space (hot regions) but not in other (cold) regions. In order to investigate this effect we study the imaginary part of the self-energy, plotted in Fig. 2. Using Eq. (1), we can evaluate the lifetime, or inverse scattering rate $\tau_k^{-1} = -\,\mathrm{Im}\Sigma(k, \omega = 0^+)$ (again extrapolating to zero the Matsubara values). Let us emphasize that our calculation is performed at a finite effective temperature. In a Fermi liquid this quantity would be small and vanish as T^2 as the temperature goes to zero. Here we find a strong modulation of τ_k^{-1} in the Brillouin zone that develops when the Mott point is approached. Our results, as well as the QMC-CDMFT of Ref. [11], may be interpreted in terms of a strongly anisotropic coherence scale, which decreases at low doping. When the scale becomes smaller than the energy resolution of our calculation we cannot follow the decrease of $\mathrm{Im}\Sigma$ with decreasing frequency (as evidenced by the line for $n = 0.98$ for $t'/t = -0.3$ of Fig. 2). Therefore it is impossible to resolve whether the Fermi liquid picture breaks down or the coherence scale is smaller than our resolution.

In Fig. 5 we show an intensity plot of τ_k^{-1} for $n = 0.9$–0.94 and the values of t' previously considered. We observe that, approaching the MT, the scattering rate is enhanced in the region around the (π, π) point of the momentum space, independently of the value of t'. This point is reminiscent of the incoherent metal behavior present in single-site studies [5], but the inclusion of the cluster impurity now allows one to differentiate the behavior of the other regions in the BZ. The FS (dashed line in Fig. 5) reaches the region of large scattering rates located around the (π, π) point at different places, according to its holelike or electronlike curvature. Hence the finite temperature lifetime is strongly modulated in momentum space. Extrapolating to zero temperature, quasiparticles disappear first in some regions of the momentum space and survive in others. In the holelike case ($t' = -0.3t$) the FS hits the large scattering region around $(0, \pi)$ and $(\pi, 0)$, while for the electronlike cases ($t' = +0.3, 0.9$) the crossing occurs close to $(\pi/2, \pi/2)$. Thus the combined effect of different scattering properties in the momentum space and the renormalization of the FS gives rise to the formation of a cold [hot] spot in $(\pi/2, \pi/2)$ [$(0, \pi), (\pi, 0)$] in the holelike system. In the electron-doped system, the position of hot and cold spots is inverted. The presence of hot or cold regions is reflected also by the spectral function

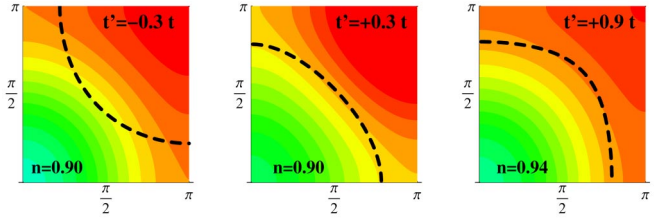

FIG. 3 (color online). $A(k, \omega = 0^+)$ in the first quadrant of the Brillouin zone. In the first row from the top $t' = -0.3t$, densities $n = 0.73, 0.89, 0.96$, color scale $x = 0.28, 0.22, 0.12$; in the second row $t' = +0.3t$, $n = 0.70, 0.90, 0.95$, color scale $x = 0.82, 0.34, 0.27$; in the lowest row $t' = +0.9t$, $n = 0.69, 0.92, 0.96$, color scale $x = 0.90, 0.32, 0.22$. The white dashed line is the FS given by $t_{\mathrm{eff}}(k) = \mu$.

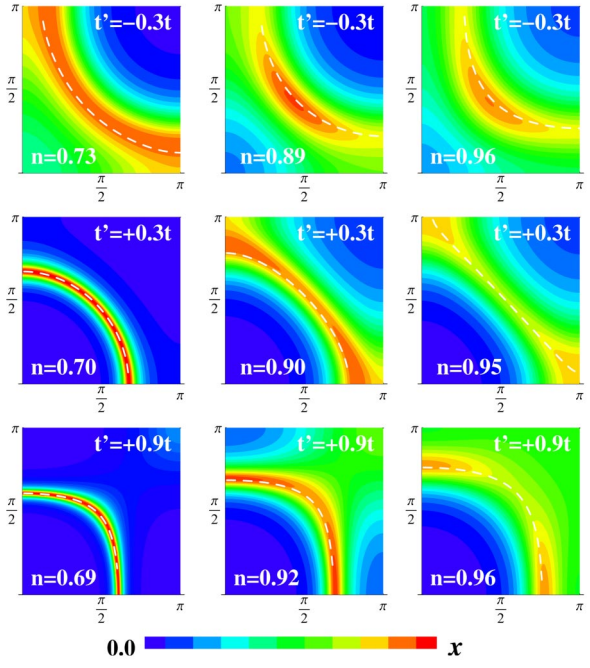

FIG. 4 (color online). Renormalization of the hopping coefficients and of their ratio as a function of density for $t'/t = \pm 0.3$.

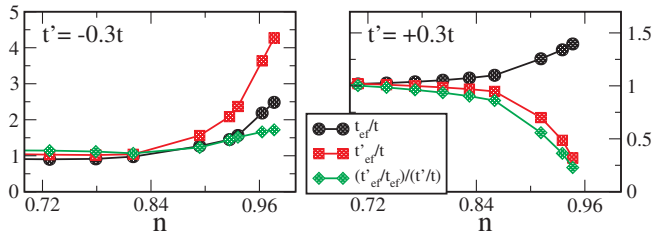

FIG. 5 (color online). τ_k^{-1} in the first quadrant of the BZ as calculated from Eq. (1). Regions around (π, π) (red) are high scattering, and around $(0, 0)$ (green) low scattering. Color scale is relative. The dashed line is the renormalized FS given by $t_{\mathrm{eff}}(k) = \mu$.

$A(k, \omega = 0^+) = -(1/\pi)\,\mathrm{Im}G(k, 0^+)$, shown in Fig. 3, which agrees with the qualitative behavior of experimental ARPES spectra [10]. These results have direct experimental implications: in particular, the analysis of photoemission data should take into account the renormalization of the FS in order to extract the model Hamiltonian parameters. They also suggest a new viewpoint on the origin of the experimentally observed asymmetry between electron and hole-doped cuprates. In the hole-doped case the quasiparticles survive in the diagonal of the Brillouin zone, near $(\pi/2, \pi/2)$, while a pseudogap opens around $(\pi, 0)$ and $(0, \pi)$. This state, which has a fermionic spectrum with point zeros can be smoothly connected to the quasiparticles of the d-wave superconducting state, whose node is close to $(\pi/2, \pi/2)$. The electron-doped case is completely different. The FS is renormalized towards nesting, stabilizing the Néel phase over a wide range of doping. Quasiparticles survive in a small region around $(\pi, 0)$ and $(0, \pi)$, and a pseudogap opens close to $(\pi/2, \pi/2)$. These quasiparticles cannot be easily deformed into the d-wave superconducting state, as in the hole-doped case, and a much larger doping is needed to reach the superconducting phase. These properties of asymmetry between the electron and hole-doped normal state of the Hubbard model have a striking resemblance to what is observed in the cuprate superconductors.

Finally, our results for large frustration $t' = +0.9t$ (right-hand panel in Fig. 5 and bottom row in Fig. 3) are always qualitatively similar to the weakly frustrated system with the same sign of t'. This shows that, at the k resolution considered in this Letter, the momentum-space differentiation does not depend on the AFM ordering of the parent insulator, as also inferred in local-approximation-based studies [5], since it occurs also for a system in which AFM is destroyed by frustration and the insulator is likely to have a more exotic form of long-range order. Moreover, since at high doping (or temperature) we find that nonlocal self-energies are negligible and single-site DMFT is not corrected by cluster DMFT, we expect similarly that there is an intermediate doping (or temperature) region where the results of the 2×2 cluster will not be modified by increasing the cluster size. In this region there is k-space differentiation, which is independent of the value of t' and is therefore due to short-range correlations, captured within the plaquette, rather than to the specific order of the parent MI.

In summary, close to the MT (i) the FS is strongly renormalized by the interaction, (ii) the FS breaks down into cold or hot regions, whose precise location is the result of an interplay of the renormalization of the real and the imaginary parts of the self-energy, (iii) the emergence of these hot or cold regions is a consequence of the proximity to the MT rather than to a long-ranged AFM state.

We thank K. M. Shen, Z.-X. Shen, P. Armitage, and A. Fujimori for sharing experimental results, and A.-M. Tremblay, D. Sénéchal, B. Kyung, T. Stanescu, C. Castellani, and A. Georges for useful discussions. M. Ca. acknowledges Italian MIUR Cofin 2003 and the NSF support under Grant No. DMR-0096462, and S. S. K. the NSERC (Canada), FQRNT (Quebec), and CFI (Canada). O. P. acknowledges the support under an ACI grant of French Ministry of Research.

[1] P. W. Anderson, Science **235**, 1196 (1987).
[2] A. Georges *et al.*, Rev. Mod. Phys. **68**, 13 (1996).
[3] G. Kotliar *et al.*, Phys. Rev. Lett. **87**, 186401 (2001).
[4] Th. Maier *et al.*, Phys. Rev. Lett. **85**, 1524 (2000); A. I. Lichtenstein and M. I. Katsnelson, Phys. Rev. B **62**, R9283 (2000).
[5] O. Parcollet and A. Georges, Phys. Rev. B **59**, 5341 (1999); K. Haule *et al.*, Phys. Rev. Lett. **89**, 236402 (2002); K. Haule *et al.*, Phys. Rev. B **68**, 155119 (2003); T. D. Stanescu and P. Phillips, Phys. Rev. Lett. **91**, 049901(E) (2003).
[6] M. Caffarel and W. Krauth, Phys. Rev. Lett. **72**, 1545 (1994).
[7] M. Grilli and G. Kotliar, Phys. Rev. Lett. **64**, 1170 (1990); G. Kotliar and J. Liu, Phys. Rev. B **38**, R5142 (1988).
[8] M. Capone *et al.*, Phys. Rev. B **69**, 195105 (2004).
[9] B. Kyung *et al.*, cond-mat/0502565.
[10] A. Damascelli *et al.*, Rev. Mod. Phys. **75**, 473 (2003); J. C. Campuzano *et al.*, in *Physics of Superconductors*, edited by K. H. Bennemann and J. B. Ketterson (Springer, Berlin, 2004), Vol. II, pp. 167–273.
[11] O. Parcollet *et al.*, Phys. Rev. Lett. **92**, 226402 (2004).
[12] Th. A. Maier *et al.*, Phys. Rev. B **66**, 075102 (2002); T. Tohyama and S. Maekawa, Phys. Rev. B **49**, 3596 (1994); C. Kusko *et al.*, Phys. Rev. B **66**, 140513(R) (2002); D. Sénéchal and A.-M. S. Tremblay, Phys. Rev. Lett. **92**, 126401 (2004); B. Kyung *et al.*, Phys. Rev. Lett. **93**, 147004 (2004); F. H. L. Essler and A. M. Tsvelik, Phys. Rev. B **65**, 115117 (2002); H. Kusunose and T. M. Rice, Phys. Rev. Lett. **91**, 186407 (2003).
[13] D. Sénéchal D. Perez, and D. Plouffe, Phys. Rev. B **66**, 075129 (2002).
[14] T. D. Stanescu and G. Kotliar (to be published).
[15] K. M. Shen *et al.*, Science **307**, 901 (2005).